Applied Physics Letters ARTICLE pubs.aip.org/aip/apl

How backreflection contributes to light absorption for high-performance radial junction photovoltaics

Cite as: Appl. Phys. Lett. **123**, 231102 (2023); doi: 10.1063/5.0174700
Submitted: 1 September 2023 · Accepted: 23 October 2023 ·
Published Online: 4 December 2023

Shaobo Zhang,[1,a)] Shuyi Wang,[2] Ruijin Hu,[1] Yunqing Cao,[1] Junzhuan Wang,[2] Jun Xu,[2] and Linwei Yu[2,a)]

AFFILIATIONS

[1]College of Physical Science and Technology/Microelectronics Industry Research Institute, Yangzhou University, 225002 Yangzhou, People's Republic of China
[2]School of Electronics Science and Engineering/National Laboratory of Solid State Microstructures/Collaborative Innovation Center of Advanced Microstructures, Nanjing University, 210023 Nanjing, People's Republic of China

[a)]**Authors to whom correspondence should be addressed:** shaobozhang@yzu.edu.cn and yulinwei@nju.edu.cn

ABSTRACT

A robust radial junction (RJ) structure directly constructed upon the surface of a flexible Al foil substrate shows a promising potential to boost wearable and portable applications, where the silicon nanowire (SiNW) supported multilayer has proven beneficial in excellent mechanical stability and sufficient light harvesting. Assigned to the beneficial backreflection contributed by the Al foil, a much larger light current can be achieved than that on glass. While a comprehensive understanding of the light absorption under the backreflection of the substrate remains mainly unexplored. Herein, a straightforward comparison of light absorption of RJ units on Al and glass substrates, within a theoretical framework based on a finite-element simulation, is performed. Then, taking SiNW geometric parameters and *i*-layer thickness into account, the evolutions of light harvesting and the external quantum efficiency curves are systematically studied. These results indicate that, under the backreflection of the substrate, the light absorption shows a reduced dependency on SiNW geometry and *i*-layer thickness to some extent, laying a critical basis to establish a simpler/easier fabrication process for high-performance flexible RJ thin film photovoltaics.

By integrating vertical silicon nanowire (SiNW) into industrial-mature thin film photovoltaic technology, the light-weight and flexible radial *p–i–n* junction (RJ) hydrogenated amorphous Si (a-Si:H) thin film photovoltaics can be directly constructed upon the surface of flexible substrates, accomplished with an excellent power-to-weight ratio for wearable/portable applications.[1–4] By comparing with the conventional planar a-Si:H thin films deposited on flexible substrates, which easily leave bending-induced large cracks and peeling-off,[5–7] the vapor–liquid–solid (VLS) grown SiNW framework can act as firmly anchor sites to host the subsequently deposited a-Si:H thin film, protecting the working region far away from the stress-rich surface of flexible substrates undergoing mechanical bending.[1,2,8,9] Remarkably, by taking low-melting-point metals as catalysts, such as tin (Sn), indium (In), gallium (Ga), bismuth (Bi), and their alloy,[10–15] the fabrication temperature of VLS-grown SiNWs can be largely reduced down to 350 °C in a plasma-enhanced chemical vapor deposition (PECVD) system. Thus, such low temperatures make it possible to construct very flexible and mechanically stable RJ-structured photovoltaics directly upon extremely flexible and low-cost Al foil substrate,[1,2,4] which is compatible with the large-scale roll-to-roll technology.[16,17]

Notably, a much larger short-circuit light current density (J_{sc} of 14.2 mA/cm^2, measured under AM1.5G illumination) can be achieved, partially assigned to the beneficial backreflection contributed by the Al foil substrate, compared to the J_{sc} of 11.8 mA/cm^2 on the AZO glass substrate fabricated in the same batch.[1] Such backreflection of the substrate would play an important role in determining light absorption of RJs, which is an interesting issue. Though several works have addressed the light in-coupling and absorption profile in complex multilayer *p–i–n* thin film solar cell structures,[18–20] the effect of backreflection and its implications for device performance remain unexplored. The radially stacked multilayer RJ unit can be seen as a 1D-cavity-like composite, where photonic and resonant mode matching effects via optical antenna coupling or leaky-mode-resonance can play an important role in determining light absorption and scattering, which have been observed experimentally in RJ solar cells.[21,22] How this scattering, under the backreflection of the substrate, will affect the light harvesting

behavior in the RJ thin film solar cell remains an important/interesting issue to address. In addition, the SiNW geometry design has to be taken into account seriously, in choosing the best trade-off between efficient carrier collection and sufficient light absorption, especially whether the backreflection can help.

In this work, we will first perform a straightforward comparison of light absorption of RJ units on Al/glass substrates, within a theoretical framework based on a finite-element simulation, emphasizing/identifying the benefit of backreflection. Then, we will explore the evolutions of light harvesting behavior and the calculated external quantum efficiency (EQE) curves, under different SiNW lengths (L_w), radius (R_w), densities, and intrinsic light absorber thickness (T_i), respectively. Our results show that, with the contribution of the backreflection of the Al substrate, the variations of SiNW geometry and light absorber thickness have a smaller influence on the light absorption of RJ units, compared to that on the glass substrate, which can help to easily find a trade-off between an optimal SiNW geometry for sufficient absorption and a higher quality of a sidewall-deposited thin film for efficient carrier collection, establishing a simpler/easier fabrication process for high-performance flexible RJ thin film solar cells.

The fabrication process of RJ thin film solar cells has been carefully described in our previous works.[12,23,24] According to the SEM images [Figs. S1(a)–S1(c)], the modeling for simulation is built, as shown in Figs. S1(d) and S1(e). Taking the geometrical dimensions (L_w, R_w, density) and T_i of RJs into account, we have performed a finite element simulation on the light absorption within a periodic matrix of RJs on Al and glass substrates, by using the RF module of COMSOL analysis toolkit. The n–k curves for each material layer are extracted via the spectroscopic ellipsometry measurement (see supplementary material S1 in Ref. 18). Note that, to focus on the contribution arising from the SiNW-supported RJ units, the bottom planar p–i–n junction layer (the planar part between RJ units) has been removed in all the simulations performed hereafter, and for the sake of simplicity.

The spatial absorption power distribution realized within the i-layer can be extracted by

$$P_{abs} = c \cdot I_{in} \cdot 4\pi k/\lambda,$$

where c is the light speed in vacuum, k is the imaginary part of refractive index $\tilde{n} = n + ik$, and $I_{\text{in}} = \varepsilon E^2/2$ is the local electromagnetic energy density.

By integrating the power dissipation losses within a selected volume of each material layer and normalizing them with respect to the total power of the incident light field, the percentage of effective power absorption realized within the i-layer can be calculated by

$$W_i = \int_{i-\text{layer}} P_{\text{abs}} \text{dv} / P_{\text{incident}},$$

where $P_{\text{incident}} = \int_{\text{top}-\text{plane}} \frac{1}{2} c \cdot \varepsilon \cdot E^2 ds$.

Assuming that the absorption of one photon generates only one electron–hole pair, the effective absorption power of $W_i^{a-Si:H}$ corresponds to an upper bound of the EQE of the thin film solar cells (excluding recombination issues).

Figure 1(a) shows a side-view SEM image of final-fabricated RJ units, where a radially stacked multilayer structure is made up of

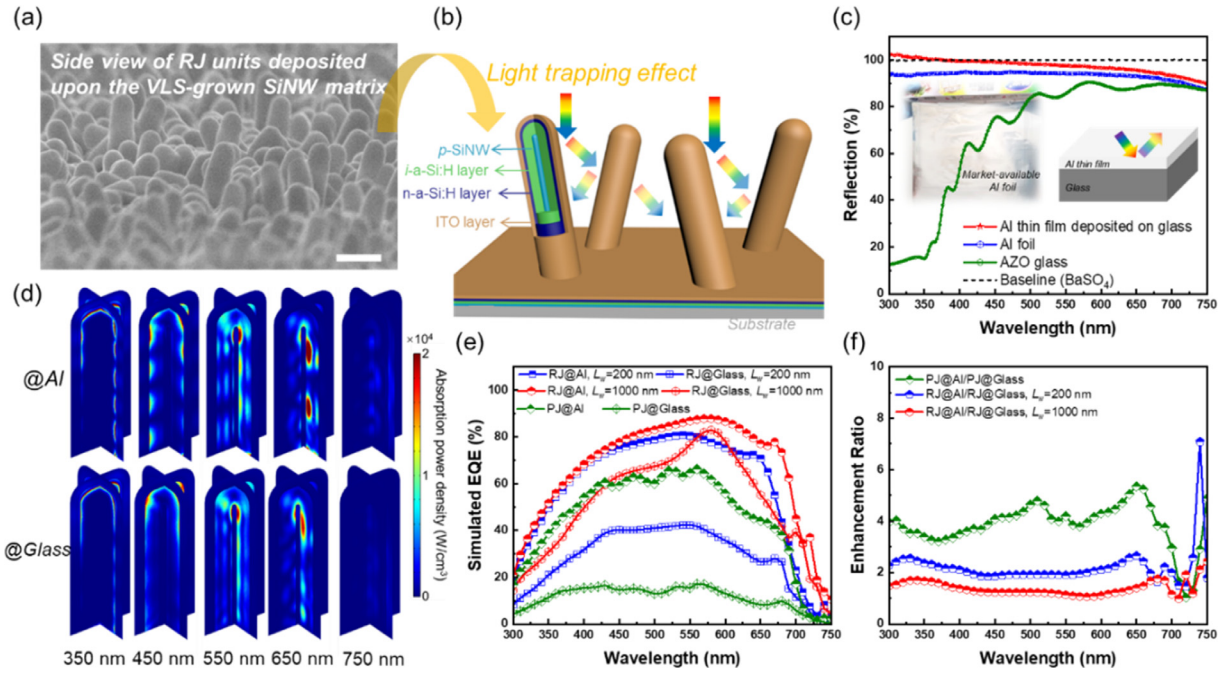

FIG. 1. (a) Side-view SEM images of RJ units. (b) Diagram of final RJ configuration. (c) Spectrum of light reflection of the Al thin film deposited on glass, Al foil as well as AZO glass. (d) Simulated light absorption profiles of RJs on Al and glass substrates (L_w is 800 nm, W_{sub} is 800 nm, R_w is 20 nm, T_i is 120 nm), respectively. (e) Simulated EQE curves of RJ units on Al and glass substrates (W_{sub} is 800 nm, R_w is 20 nm, T_i is 120 nm), respectively, as well as PJ references. (f) The spectrum of EQE enhancement ratio extracted from (e). The scale bar is 400 nm in (a).

p-SiNW, intrinsic a-Si:H layer, n-type a-Si:H layer, and transparent ITO layer, as drawn schematically in Fig. 1(b). The light reflection curves of the Al thin film deposited on glass, Al foil, and Al-doped zinc oxide (AZO) glass are presented in Fig. 1(c), directly showing a larger reflection of Al foil or Al thin film substrates than the AZO glass substrate. Figures 1(d) and S2 show the simulated light absorption patterns extracted from normal-section and cross section surfaces of RJ units on Al and glass substrates, under different wavelengths from 350 to 750 nm. As we can see, the most absorption of short wavelengths (<450 nm) happens only superficially at the outer shells (ITO and n-type a-Si:H layers), with only a small fraction reaching the intrinsic light absorber, while longer wavelengths (>550 nm) have deeper penetration depth into the RJ units. With the contribution of the backreflection of the Al substrate, enhanced light absorption can be observed, especially at the bottom of RJs (Fig. S2). The simulated EQE curves of RJ units on Al and glass substrates with L_w of 200 and 1000 nm are shown in Fig. 1(e), respectively. In addition, the planar junctions (PJs, with the same *i*-layer thickness) on Al and glass substrates are taken as references, where the built model for simulation has an area roughly equal to the cross section area of radial *p–i–n* junction because the planar part between the RJ units has been removed for the sake of simplicity, thus contributing to a very low EQE of the PJ on the glass substrate. Thanks to the backreflection of Al substrate, the simulated EQE curves on Al substrates are better than those on glass substrates, which can be directly observed from the spectrum of EQE enhancement ratio [Fig. 1(f)]. We note that the value of the enhancement ratio is >1 over the full spectrum, and at the long wavelengths (especially >600 nm), some fluctuations exist, which is consistent with the variation trend of light reflection curves shown in Fig. 1(c). Interestingly, as the L_w increases, the overall EQE enhancement ratio decreases, which can be attributed to the enhanced light trapping effect among RJ units, as shown in Fig. 1(b), largely increasing the light absorption path and reducing the light intensity arrived at the surface of substrates. To verify the contribution of the light trapping effect realized among the SiNW framework, a comparison of the simulated EQE responses is presented in Fig. S3. At the short wavelengths (from 350 to 550 nm), the values of the EQE enhancement ratio of RJ units on Al substrates are almost the same; as to the long wavelengths (550 to 750 nm), the EQE enhancement ratio of RJ/PJ ($L_w \sim 1000$ nm) has an obvious increase. This seems that during short wavelengths, the backreflection of Al substrates plays a dominant role, while at the long wavelengths, the light scattering among 3D architecture is still prominent. Thus, how and to what extent the backreflection of substrates can help to simplify SiNW geometry design and easily seek an optimal light harvesting performance could be an intriguing issue to explore.

The L_w is an important geometry parameter to adjust 3D RJ thin film solar cells. Figures 2(a) and 2(b) show the simulated EQE curves of RJ units with different L_w on Al and glass substrates, respectively, as well as the simulated light absorption patterns shown in Fig. S4. As the L_w increases, there is an overall enhancement of EQE curves for the incident wavelengths >550 nm, while at the short wavelengths, the absorption enhancement is almost the same for the Al substrate and

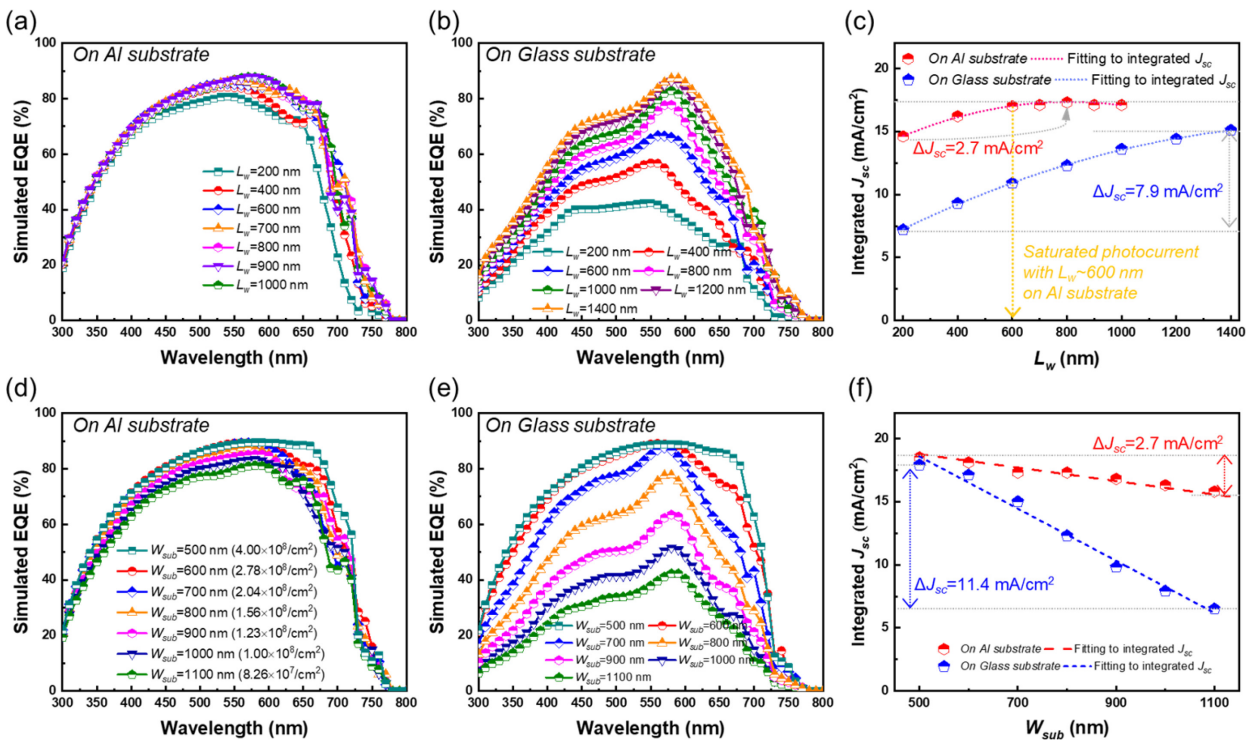

FIG. 2. (a) and (b) Simulated EQE curves of RJ units with different L_w on Al and glass substrates (W_{sub} is 800 nm, R_w is 20 nm, T_i is 120 nm), respectively. (c) Integrated J_{sc} from simulated EQE of RJ units on Al and glass substrates, respectively. (d) and (e) Simulated EQE curves of RJs on Al and glass substrates with different W_{sub} (different densities of RJ units, L_w is 800 nm, R_w is 20 nm, T_i is 120 nm), respectively. (f) Integrated J_{sc} from simulated EQE curves of RJ units on Al and glass substrates, respectively.

varies slightly for the glass substrate, as shown in Fig. S5. Figure 2(c) shows the integrated J_{sc} from the simulated EQE curves. It is found that, on the Al substrate, the integrated J_{sc} increases gradually with L_w before saturating at $L_w \sim 600$ nm and above, with a saturated value of $\sim$17.1 mA/cm^2, while the J_{sc} obtained on glass substrates exhibit a monotonic increase trend with increasing L_w. The saturated value of J_{sc} of RJs on the Al substrate is just 2.7 mA/cm^2 larger than that of RJs with $L_w \sim 200$ nm. However, even if the L_w reaches 1400 nm, the J_{sc} of RJs on the glass substrate is just 15.1 mA/cm^2, which is smaller than the saturated one on the Al substrate. A conclusion can be drawn that with the contribution of the backreflection of the substrate, too long L_w is not necessary, which will help to achieve a better quality of thin film deposited on the sidewall of SiNW for a better carrier collection.

Another important geometry parameter is the density of SiNWs, which plays an important role in light scattering of such 3D architecture. Figures S6(a) and S6(b) show the top-view SEM images of a sparse RJ matrix with a density of 1.1×10^8/cm^2 and a dense RJ matrix with a density of 3.1×10^8/cm^2, respectively. Taking the 3 nearest RJs as examples to measure the distance, it is clear that a dense RJ matrix has a smaller distance among RJ units, which can be represented by the width of the cubic simulation box (W_{sub}) in the model; thus, we perform the density-changed simulation of RJ units by changing W_{sub}. The simulated EQE curves of RJ units on Al and glass substrates are shown in Figs. 2(d) and 2(e), respectively, as well as the simulated light absorption patterns presented in Fig. S7. It can be seen that, as the W_{sub} increases, there is an obvious decline of EQE curves on the glass substrate, while for the RJ units on the Al substrate, the variations of EQE curves are rather slight. The integrated J_{sc} values are shown in Fig. 2(f). When the W_{sub} is changed from 500 to 1100 nm (the corresponding density of RJ units is changed from 4.00×10^8/cm^2 to 8.26×10^7/cm^2), the integrated J_{sc} of RJ units on the Al substrate has a slight decline of 2.7 mA/cm^2, which is much smaller than that (11.4 mA/cm^2) of ones on the glass substrate. For a deeper understanding, the integrated J_{sc} values are calculated in the wavelength range of 300–550 nm or 550–800 nm, respectively, as shown in Fig. S6(c). It is interesting to note that the decline of an overall J_{sc} on the Al substrate can be largely attributed to the relatively larger decline of integrated J_{sc} from long wavelength, which is mainly influenced by the light scattering, where the RJ unit can harness the incident light over a cross-sectional area much larger than its physical diameter, that is, the incident light can be more effectively collected into the 1D-cavity-like RJ cell.[25,26] A similar trend can be observed in the samples on the glass substrate. As to the variations of the radii of SiNW (R_w), the influence of variations of R_w on the light absorption of RJ units on Al or glass substrates can be almost negligible, as shown in Figs. S6(d)–S6(f).

Furthermore, as defined in Fig. 3(a), the influence of i-layer thickness (T_i) on light harvesting of RJs on Al and glass substrates has been studied. The simulated light absorption patterns of RJ units with different T_i are shown in Fig. S8. At the longer wavelengths ($\lambda > 550$ nm), the incident light field propagates deeper into the light absorber of the RJ unit, benefiting from a strong resonant-mode enhanced in-coupling into such a quasi-1D RJ antenna.[18] It is interesting to see that, at the same wavelength, the incident light field can propagate much deeper in a thinner absorber than a thicker one, as shown in Fig. S8. Figures 3(b) and 3(c) show the simulated EQE curves as well as the integrated J_{sc} as a function of T_i in Fig. 3(d). With the contribution of backreflection,

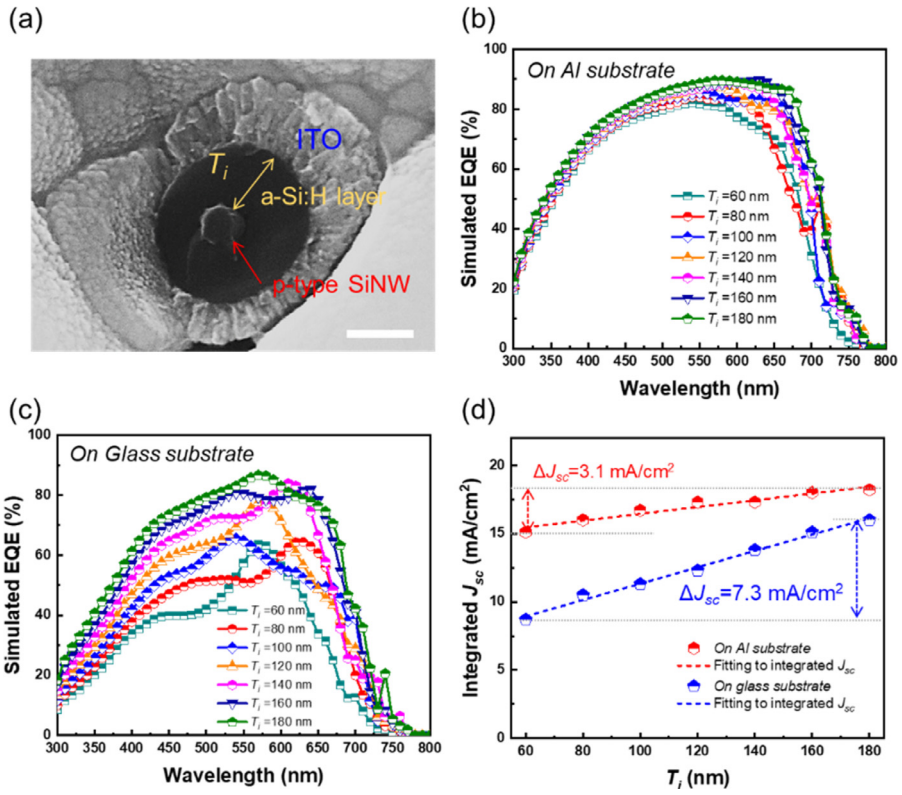

FIG. 3. (a) Cross-sectional SEM images of RJ units. (b) and (c) Simulated EQE curves of RJ units on Al and glass substrates with different T_i (L_w is 800 nm, W_{sub} is 800 nm, and R_w is 20 nm), respectively. (d) Integrated J_{sc} from simulated EQE curves of RJ units on Al and glass substrates. The scale bar in (a) is 100 nm.

when the T_i is 60 nm, the integrated J_{sc} on the Al substrate is 15.1 mA/cm^2, which is much larger than that (8.7 mA/cm^2) on the glass substrate. As the T_i increases from 60 to 180 nm, the J_{sc} on the Al substrates augments slightly to 18.2 mA/cm^2, compared to a much larger increase in 7.3 mA/cm^2 of J_{sc} on the glass substrate. With the T_i increases, the contribution of backreflection becomes weaker, as shown in Fig. S9 (the spectrum of EQE enhancement ratio). However, the too-thick absorber is a barrier to efficiently collecting carriers; thus, how to find a trade-off is a rather important/challenging issue.

These observations indicate that (1) the backreflection of substrates can indeed result in an overall enhancement of light absorption realized within the *i*-layer of RJ units; (2) although on the Al substrate, the light harvesting performance at the long wavelength is still mainly determined by light scattering but this function is weakened by the backreflection, compared to RJ units on the glass substrate; and (3) with the contribution of the backreflection of the substrate, the influence of variations of SiNW geometry, especially L_w and density, as well as T_i, on the EQE values becomes less.

In summary, we have performed a comprehensive investigation on the impacts of backreflection of the substrate, by examining the simulated absorption patterns and calculating the EQE curves. We found that the light harvesting realized by RJ units can be largely enhanced by the backreflection of the substrate, which can weaken but not completely supplant the influence of light scattering among 3D architecture. It should be pointed out that the contribution arising from the backreflection of the substrate can help the light absorption of RJ units to reduce the dependency on SiNW geometry and light absorber thickness to some extent, making it possible to decouple sufficient light harvesting from SiNW geometry. These results have provided a unique perspective and practical guide in seeking an easier/simpler process to fabricate high-performance flexible RJ thin film photovoltaics on metal foil substrate compatible with roll-to-roll technology.

See the supplementary material for the built geometry for COMSOL simulation, the simulated light absorption patterns, and some EQE enhancement ratio curves.

The authors acknowledged the financial supports from the National Key Research Program of China under Grant No. 92164201, National Natural Science Foundation of China for Distinguished Young Scholars No. 62325403, National Natural Science Foundation of China under No. 61974064, Special Fund for City School Cooperation of Yangzhou City (No. YZ2022177), and Innovation technology platform project jointly built by Yangzhou City and Yangzhou University (No. YZ2020268).

AUTHOR DECLARATIONS

Conflict of Interest

The authors have no conflicts to disclose.

Author Contributions

Shaobo Zhang: Conceptualization (lead); Data curation (lead); Formal analysis (lead); Investigation (lead); Methodology (lead); Writing – original draft (lead); Writing – review & editing (lead). **Shuyi Wang:** Data curation (equal); Formal analysis (supporting); Investigation (supporting); Methodology (equal); Validation (equal); Visualization (supporting). **Ruijing Hu:** Data curation (supporting); Formal analysis (supporting); Funding acquisition (supporting); Investigation (supporting); Methodology (supporting); Resources (supporting); Writing – original draft (supporting). **Yunqing Cao:** Formal analysis (supporting); Funding acquisition (supporting); Investigation (supporting); Resources (supporting). **Junzhuan Wang:** Formal analysis (supporting); Funding acquisition (equal); Methodology (supporting); Resources (supporting); Software (lead); Writing – review & editing (supporting). **Jun Xu:** Funding acquisition (supporting); Resources (supporting); Writing – review & editing (supporting). **Linwei Yu:** Conceptualization (lead); Data curation (equal); Formal analysis (equal); Funding acquisition (lead); Investigation (equal); Project administration (equal); Resources (lead); Software (lead); Supervision (lead); Visualization (equal); Writing – original draft (equal); Writing – review & editing (lead).

DATA AVAILABILITY

The data that support the findings of this study are available from the corresponding authors upon reasonable request.

REFERENCES

[1]X. Sun, T. Zhang, J. Wang, F. Yang, L. Xu, J. Xu, Y. Shi, K. Chen, P. Roca i Cabarrocas, and L. Yu, "Firmly standing three-dimensional radial junctions on soft aluminum foils enable extremely low cost flexible thin film solar cells with very high power-to-weight performance," Nano Energy **53**, 83–90 (2018).
[2]S. Zhang, T. Zhang, Z. Liu, J. Wang, J. Xu, K. Chen, and L. Yu, "Flexible and robust 3D a-SiGe radial junction near-infrared photodetectors for rapid sphygmic signal monitoring," Adv. Funct. Mater. **32**, 2107040 (2022).
[3]S. Zhang, T. Zhang, Z. Liu, J. Wang, L. Yu, J. Xu, K. Chen, and P. Roca i Cabarrocas, "Highly flexible radial tandem junction thin film solar cells with excellent power-to-weight ratio," Nano Energy **86**, 106121 (2021).
[4]Z. Liu, B. Wen, L. Cao, S. Zhang, Y. Lei, G. Zhao, L. Chen, J. Wang, Y. Shi, J. Xu, X. Pan, and L. Yu, "Photoelectric cardiac pacing by flexible and degradable amorphous Si radial junction stimulators," Adv. Healthcare Mater. **9**, 1901342 (2020).
[5]C. Hengst, S. B. Menzel, G. K. Rane, V. Smirnov, K. Wilken, B. Leszczynska, D. Fischer, and N. Prager, "Mechanical properties of ZTO, ITO, and a-Si:H multilayer films for flexible thin film solar cells," Materials **10**, 245 (2017).
[6]W. J. Dong, C. J. Yoo, H. W. Cho, K.-B. Kim, M. Kim, and J.-L. Lee, "Flexible a-Si:H solar cells with spontaneously formed parabolic nanostructures on a hexagonal-pyramid reflector," Small **11**, 1947–1953 (2015).
[7]Q. Lin, L. Lu, M. M. Tavakoli, C. Zhang, G. C. Lui, Z. Chen, X. Chen, L. Tang, D. Zhang, Y. Lin, P. Chang, D. Li, and Z. Fan, "High performance thin film solar cells on plastic substrates with nanostructure-enhanced flexibility," Nano Energy **22**, 539–547 (2016).
[8]X. Xie, X. Zeng, P. Yang, H. Li, J. Li, X. Zhang, and Q. Wang, "Radial n-i-p structure SiNW-based microcrystalline silicon thin-film solar cells on flexible stainless steel," Nanoscale Res. Lett. **7**, 621 (2012).
[9]X. Xie, X. Zeng, P. Yang, H. Li, J. Li, X. Zhang, and Q. Wang, "Radial n-i-p structure silicon nanowire-based solar cells on flexible stainless steel substrates," Phys. Status Solidi A **210**, 341–344 (2013).
[10]L. Yu, B. O'Donnell, P. J. Alet, S. Conesa-Boj, F. Peiro, J. Arbiol, and P. Roca i Cabarrocas, "Plasma-enhanced low temperature growth of silicon nanowires and hierarchical structures by using tin and indium catalysts," Nanotechnology **20**, 225604 (2009).
[11]I. Zardo, L. Yu, S. Conesa-Boj, S. Estrade, P. J. Alet, J. Rossler, M. Frimmer, P. Roca i Cabarrocas, F. Peiro, J. Arbiol, J. R. Morante, and I. M. A. Fontcuberta, "Gallium assisted plasma enhanced chemical vapor deposition of silicon nanowires," Nanotechnology **20**, 155602 (2009).
[12]L. Yu, F. Fortuna, B. O'Donnell, T. Jeon, M. Foldyna, G. Picardi, and P. Roca i Cabarrocas, "Bismuth-catalyzed and doped silicon nanowires for one-pump-down fabrication of radial junction solar cells," Nano Lett. **12**, 4153–4158 (2012).

[13]Z. Yu, J. Lu, S. Qian, S. Misra, L. Yu, J. Xu, L. Xu, J. Wang, Y. Shi, K. Chen, and P. Roca i Cabarrocas, "Bi-Sn alloy catalyst for simultaneous morphology and doping control of silicon nanowires in radial junction solar cells," Appl. Phys. Lett. **107**, 163105 (2015).
[14]L. Yu, F. Fortuna, B. O'Donnell, G. Patriache, and P. Roca i Cabarrocas, "Stability and evolution of low-surface-tension metal catalyzed growth of silicon nanowires," Appl. Phys. Lett. **98**, 123113 (2011).
[15]L. Yu, B. O'Donnell, J.-L. Maurice, and P. Roca i Cabarrocas, "Core-shell structure and unique faceting of Sn-catalyzed silicon nanowires," Appl. Phys. Lett. **97**, 023107 (2010).
[16]O. Keles and M. Dundar, "Aluminum foil: Its typical quality problems and their causes," J. Mater. Process. Technol. **186**, 125–137 (2007).
[17]S.-F. Leung, L. Gu, Q. Zhang, K.-H. Tsui, J.-M. Shieh, C.-H. Shen, T.-H. Hsiao, C.-H. Hsu, L. Lu, D. Li, Q. Lin, and Z. Fan, "Roll-to-roll fabrication of large scale and regular arrays of three-dimensional nanospikes for high efficiency and flexible photovoltaics," Sci. Rep. **4**, 4243 (2014).
[18]L. Yu, S. Misra, J. Wang, S. Qian, M. Foldyna, J. Xu, Y. Shi, E. Johnson, and P. Roca i Cabarrocas, "Understanding light harvesting in radial junction amorphous silicon thin film solar cells," Sci. Rep. **4**, 4357 (2014).
[19]J. Lu, S. Qian, Z. Yu, S. Misra, L. Yu, J. Xu, Y. Shi, P. Roca i Cabarrocas, and K. Chen, "How tilting and cavity-mode-resonant absorption contribute to light harvesting in 3D radial junction solar cells," Opt. Express **23**, A1288–1296 (2015).
[20]S. Qian, S. Misra, J. Lu, Z. Yu, L. Yu, J. Xu, J. Wang, L. Xu, Y. Shi, K. Chen, and P. Roca i Cabarrocas, "Full potential of radial junction Si thin film solar cells with advanced junction materials and design," Appl. Phys. Lett. **107**, 043902 (2015).
[21]P. Krogstrup, H. I. Jùrgensen, M. Heiss, O. Demichel, J. V. Holm, M. Aagesen, J. Nygard, and A. Fontcuberta i Morral, "Single-nanowire solar cells beyond the Shockley–Queisser limit," Nat. Photonics **7**, 306–310 (2013).
[22]N. Tavakoli and E. Alarcon-Llado, "Combining 1D and 2D waveguiding in an ultrathin GaAs NW/Si tandem solar cell," Opt. Express **27**, A909–A923 (2019).
[23]S. Zhang, T. Zhang, L. Cao, Z. Liu, J. Wang, J. Xu, K. Chen, and L. Yu, "Coupled boron-doping and geometry control of tin-catalyzed silicon nanowires for high performance radial junction photovoltaics," Opt. Express **27**, 37248–37256 (2019).
[24]S. Misra, L. Yu, M. Foldyna, and P. Roca i Cabarrocas, "High efficiency and stable hydrogenated amorphous silicon radial junction solar cells built on VLS-grown silicon nanowires," Sol. Energy Mater. Sol. Cells **118**, 90–95 (2013).
[25]L. Hu and G. Chen, "Analysis of optical absorption in silicon nanowire arrays for photovoltaic applications," Nano Lett. **7**, 3249–3252 (2007).
[26]M. D. Kelzenberg, S. W. Boettcher, J. A. Petykiewicz, D. B. Turner-Evans, M. C. Putnam, E. L. Warren, J. M. Spurgeon, R. M. Briggs, N. S. Lewis, and H. A. Atwater, "Enhanced absorption and carrier collection in Si wire arrays for photovoltaic applications," Nat. Mater. **9**, 239–244 (2010).